Проаналізовано переваги диференційного Коріолісова вібраційного гіроскопа. Виконано порівняльний аналіз чотирьох методів оброблення надмірних сигналів кутової швидкості. Актуальність досліджень зумовлена необхідністю підвищення точності сучасних вібраційних гіроскопів. Отримано методи оброблення надмірної вихідної інформації гіроскопа та вдосконалено технологію «віртуального» гіроскопа шляхом обчислювання міжканальної кореляційної матриці в он-лайн режимі, з метою підвищення точності вимірювання кутової швидкості та зменшення шумів зміщення нуля в умовах змінюваних температурних впливів

Ключові слова: диференціальний вібраційний гіроскоп, технологія «віртуального» гіроскопа, зміщення нуля, кореляційна матриця

Проанализированы преимущества дифференциального Кориолисова вибрационного гироскопа. Выполнен сравнительный анализ четырех методов обработки избыточных сигналов угловой скорости. Актуальность исследований обусловлена необходимостью повышения точности современных вибрационных гироскопов. Получены методы обработки избыточной выходной информации гироскопа и усовершенствована технология «виртуального» гироскопа путем вычисления межканальной корреляционной матрицы в он-лайн режиме с целью повышения точности измерения угловой скорости и уменьшения шумов смещения нуля в условиях изменяющихся температурных воздействий

Ключевые слова: дифференциальный вибрационный гироскоп, технология «виртуального» гироскопа, смещение нуля, корреляционная матрица

UDC 621.375
DOI: 10.15587/1729-4061.2016.75206

REDUNDANT INFORMATION PROCESSING TECHNIQUES COMPARISON FOR DIFFERENTIAL VIBRATORY GYROSCOPE

V. Chikovani
Doctor of Technical Sciences, Professor*
E-mail: v_chikovani@ukr.net
O. Sushchenko
Doctor of Technical Sciences, Professor*
E-mail: sushoa@ukr.net
H. Tsiruk
Postgraduate student*
E-mail: hanna.tsiruk@gmail.com
*Aircraft Control Systems Department
National Aviation University
Komarov ave., 1, Kyiv, Ukraine, 03058

1. Introduction

Gyroscopic angle rate sensors based on modern, for example, the fiber-optic inertial technologies are widely used in the systems of payload stabilization and dynamic object motion control. Absence of moving parts, small readiness time, high sensitivity and accuracy are advantages of such gyroscopic sensors. But gyroscopic sensors built on the fiber-optic technologies have significant mass and dimensions due to usage of receiving-transmitting units. At the same time they have high cost caused by hand operations in manufacturing. Usage of gyroscopic angle rate sensors built on MEMS-technologies is one of the basic trends of modern control systems design. Such gyroscopic sensors have a wide area of application including stabilization of platforms with information and measuring devices. Development of this type of sensors is not completed now. This process requires increasing of operating characteristics and improvement of technology of sensors manufacturing. Basic advantages of such gyroscopic sensors are simplicity of operation and low cost. But achievement of definite progress is required as to accuracy characteristics of the sensors. It should be noted that some gyroscopic sensors of this type are characterized by sufficiently high resistance to shock influence. But MEMS-gyros have some disadvantages. Their characteristics have some statistical dispersion caused by deviation of manufacturing conditions from given in the technical documentation. Furthermore, processes of separate sensors ageing have different rates. Therefore the gyroscopic sensors of this type require compensation of bias. Usually correcting units with different level of complexity are used for this purpose. It should be noted that many modern gyroscopic sensors have built-in hardware, which allows improving their characteristics. So, many gyroscopic angle rate sensors designed on the basis of MEMS-technology use built-in systems of temperature compensation. Lately, the trend of MEMS-gyros characteristics improvement by means of robust controllers takes place. Such controllers provide the robust performance of sensors in conditions of their parameters variations. These controllers are able to provide desired characteristics of stability margin, bandwidth, and stability of scale factor.

The above listed disadvantages of MEMS-gyros are eliminated in the perspective digital Coriolis vibratory Gyro (CVG) with the metallic resonator [1]. Development of this gyro is implemented by the Aircraft Control Systems Department of the National Aviation University (Kyiv, Ukraine) together with PJSC SIC Kyiv Automatic Plant (KAP) named after G. Petrovsky (Kyiv, Ukraine). Comparative analysis of gyroscopic angle rate sensors of the different types is represented in Table 1.

Table 1

Parameters of gyroscopic angle rate sensors

№	Sensor type	Technology type	Producer	Measuring range, deg/s	Band-width, Hz	Resistance to shocks, g
1	GT-46	Electro-mechanical	KAP named after G. Petrovsky, Ukraine	50	40	150
2	G20-075-100	MEMS	Gladiator Technologies, USA	75	100	500
3	SDG1000	MEMS	Systron Donner, USA	75	>100	200
4	MAG-16	MEMS	Northrop Grumman, USA	150	400	–
5	DSP-1750	Fiber-optic	KVH, USA	490	40	25
6	CVG	Vibratory	KAP named after G. Petrovsky, Ukraine	400	100	400

It should be noted that MEMS-gyros such as ADXR646, ADXR16375 of Analog Devices (USA), CRG20, CRG32P of Silicon Sensing Systems (USA) are characterized by the lower accuracy in comparison with CVG. The comparative analysis of characteristics of CVG manufactured in Ukraine with characteristics of vibratory gyro with the metallic resonator "Quaposon" of Sagem (France) has been shown some its advantages by accuracy and functional possibilities. The comparative analysis of characteristics of CVG and fiber-optic gyro DSP-3000 manufactured by KVH (USA) has shown the significant advantages by such characteristics as average failure time (almost three times), bias stability (almost three times), time of readiness to functioning mode (almost five times), and also by the functional possibilities as the fiber-optic gyros have no possibilities of functioning in some operating modes. Components and appearance of CVG are represented in Fig. 1, 2.

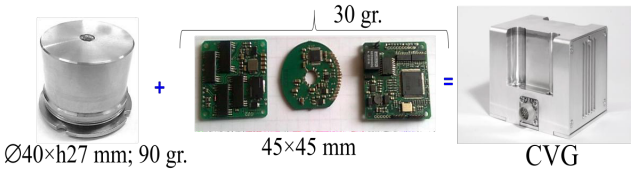

Fig. 1. Appearance of CVG

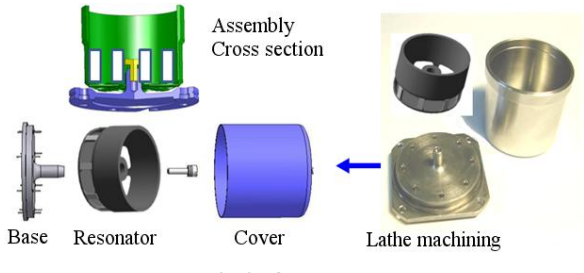

Fig. 2. CVG components

At the same time, such applications as stabilization of information and measuring devices and control of dynamic objects motion require further ways to improve accuracy of gyroscopic sensors including creation of information processing algorithms taking into consideration presence of bias due to temperature changes. Such changes are present in conditions of real operation of the systems to be researched.

Relevance of researches in the above mentioned trends lies in increasing of vibratory gyros accuracy. This provides the possibility to create the high-accurate systems of platform stabilization and control of dynamic objects motion using low cost and easy in operation inertial measuring instruments.

2. Analysis of publications data and problem statement

The problem of increasing of accuracy and decreasing of bias noise is important for all low cost MEMS-gyros and also for CVG with the metallic, piezoelectric and other types of low cost resonators. This problem requires determination of ways to design the multi-resonator sensor or array of sensors with redundant output information about angle rate of an object along one axis [2]. Integration of redundant information about angle rate, for example, by means of Kalman filter [3, 4], and extended Kalman filter [5] in complicated cases leads to the necessity of mathematical modelling of the measured angle rate. For example, the angle rate model in [6] is represented by a Markov process of the first order, and the general auto-regression model conditionally heteroscedastic model of the angle rate is used in [7]. The latter takes into consideration the temperature model of the gyro drift. It is possible also to use the model of errors based on Allan variations [8]. Based on models of angle rate, gyro errors, and Kalman filter, which integrates them, the so-called algorithm of "virtual" gyro can be created [9]. In some conditions, which are given to interconnections between different signals of sensors in an array of the "virtual" gyro, the measuring accuracy can be significantly increased. Maximum accuracy of "virtual" gyro measurements can be achieved, if equal accuracy n sensors in the array have cross-sensor correlation coefficients equal to $\rho_{opt}=-1/(n-1)$. Correlation coefficients represent non-diagonal elements of the correlation matrix. The problem lies in determination of ways to approach sensor array correlation coefficients to optimal values ρ_{opt} and implement the quantitative estimation of accuracy increase for a real gyro in the case of minimum n when n=2. From the other hand, it should be noted that CVG of the new differential type has been developed in recent years [10]. Thereupon experimental researches of capability to measure angle rate with different signs have been carried out [11]. It should be noted that gyros of this type have the great potential of accuracy increase in conditions of low cost resonators usage. The important advantage of the differential CVG is the possibility to use means of accuracy increase without changes in the process of gyro design. The single requirement is a change of control algorithm of the standing wave vibratory structure. Therefore functioning of differential CVG can be considered as the third mode of CVG operation [12] in addition to two well-known rate-integrating [13] and rate measurement [14].

The differential mode of functioning can be implemented in CVG and also in MEMS-gyros by means of keeping of standing wave position between electrodes helping applica-

tion of two signals with stable amplitude on drive electrodes X, Y. In this case, gyro output signals will present object's angle rates with opposite signs. These rates will be read from sense electrodes X, Y located for the ring resonator under the angle 45° to drive electrodes [15]. The simplest technique of information processing obtained by two measuring channels with opposite signs lies in the usage of subtraction operation $X_{sense}-Y_{sense}$ [10]. In this case, the useful signal component, which corresponds to the angle rate, increases and error components for both measuring channels are mutually eliminated. In conditions of proper alignment of standing wave angle $\theta^{*}\neq m\pi/4$, m=0, 1... components of cross-damping are compensated too.

Therefore research of the possibility to apply the known "virtual" gyro algorithm to differential CVG would have scientific and practical interest. The goal of this research is to decrease output signal noise by means of redundant information available in this signal. It would also be expedient to use specificity of differential CVG, which has two channels with opposite angle rates, to approach the cross-channel correlation coefficient to the optimal value for the minimum quantity of channels (n=2). Furthermore, creation of modified "virtual" gyro algorithm has theoretical and practical interest, as this will allow taking into consideration change of cross-channel correlation coefficient versus time during changes of environmental conditions. In particular, it would be appropriate if such modified algorithm foresaw the possibility to calculate cross-channel correlation matrix in on-line manner with approaching of the cross-channel correlation coefficient to an optimal value.

3. Research purpose and tasks

The purpose of the carried out researches was determination of ways of redundant information processing for differential type CVG.

To achieve this purpose the following tasks have been solved:

– improvement of the algorithm by on-line calculation of the correlation matrix;

– comparison of the proposed improved algorithm with the known techniques [3, 4, 10];

– determination of the condition, for which the correlation coefficient ρ approaches to an optimal value ρ_{opt};

– quantitative estimation and comparison of random and systematic errors and overshoot value during abrupt change of angle rate for application of different techniques of redundant information processing in differential CVG.

During researches the comparative analysis of four techniques of information processing from the point of view of measuring accuracy increase and bias noise decrease, when temperature changes, was carried out.

4. Research materials and different techniques for CVG redundant information processing

4. 1. Differential mode of CVG operation

Dynamic equations of standing elastic wave based on two-dimensional pendulous model [16] can be presented as follows

$$\ddot{x}-2k\Omega\dot{y}+d_{xx}\dot{x}+d_{xy}\dot{y}+k_{xx}x+k_{xy}y=f_x;$$

$$\ddot{y}+2k\Omega\dot{x}+d_{yx}\dot{x}+d_{yy}\dot{y}+k_{yx}x+k_{yy}y=f_y;$$

$$d_{xx}=2/\tau+h\cos 2\theta_\tau,\quad 2/\tau=1/\tau_1+1/\tau_2,$$

$$h=1/\tau_1-1/\tau_2,\quad d_{yy}=2/\tau-h\cos 2\theta_\tau,\quad d_{xy}=h\sin 2\theta_\tau,$$

$$k_{xx}=\omega_1^2-\omega\Delta\omega\cos 2\theta_\omega,\quad k_{yy}=\omega_2^2+\omega\Delta\omega\cos 2\theta_\omega,$$

$$\omega\Delta\omega=(\omega_1^2-\omega_2^2)/2,\quad k_{xy}=-\omega\Delta\omega\sin 2\theta_\omega, \qquad (1)$$

where k is Brian coefficient depending on resonator geometry; d_{xx} is X axis damping coefficient; τ_1 is minimum resonator's damping time; τ_2 is maximum resonator's damping time; d_{yy} is Y axis damping coefficient; $d_{xy}=d_{yx}$ are damping cross-coupling coefficients; k_{xx} and k_{yy} are normalized by mass resonator rigidities along X and Y axes, respectively; θ_ω and θ_τ are angles between minimum frequency and damping axes and standing wave antinode axis, respectively, shown in Fig. 3; ω_1, ω_2 are maximum and minimum resonant frequencies; $\Delta\omega=\omega_1-\omega_2$ is frequency mismatch; $k_{xy}=k_{yx}$ are resonator rigidity cross-coupling coefficients; f_x and f_y are normalized by mass control forces.

If believe that control forces f_x and f_y are applied to the excitation electrodes X and Y so that standing wave is positioned at an angle $\theta\neq m\pi/4$, m=0, 1, 2... to the X channel drive electrode, then they can be determined as follows

$$f_x=(K_d^x\dot{x}+K_f^x x)G_x;$$

$$f_y=(K_d^y\dot{y}+K_f^y y)G_y, \qquad (2)$$

where $K_d^x, K_f^x, K_d^y, K_f^y$ are control signals components responsible for resonator's damping and rigidity along X and Y axes expressed in electrical signals and modulated by displacements x and y and displacement rates $\dot{x}$, $\dot{y}$, respectively; G_x and G_y are transformation coefficients of control voltages applied on X and Y drive electrodes into the forces, respectively.

It should be noted that standing wave antinode does not coincide with any of eight electrodes disposed at equal angles $\pi/4$ along resonator circumferential coordinate. Four of these electrodes are shown in Fig. 3.

Substitution (2) in (1) and grouping terms results in the following equations

$$\ddot{x}+d_{xx}\dot{x}+(k_{xx}-K_f^xG_x)x+k_{xy}y=(2k\Omega-d_{xy})\dot{y}+K_d^xG_x\dot{x};$$

$$\ddot{y}+d_{yy}\dot{y}+(k_{yy}-K_f^yG_y)y+k_{xy}x=(-2k\Omega-d_{xy})\dot{x}+K_d^yG_y\dot{y}. \qquad (3)$$

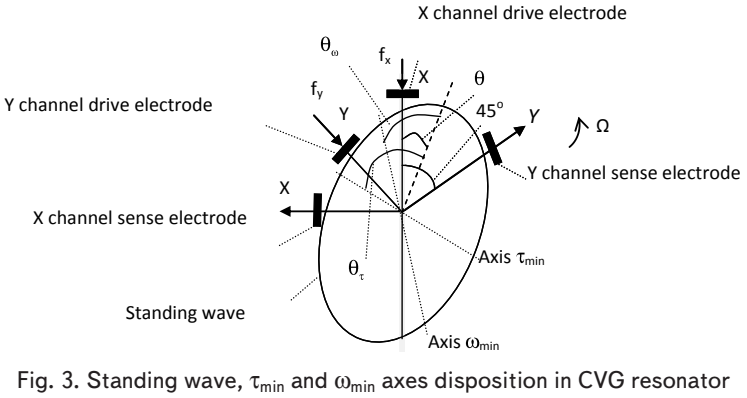

Fig. 3. Standing wave, τ_{min} and ω_{min} axes disposition in CVG resonator

Terms at x and y variables in the left side of the equations (3) are responsible for vibration frequency along X and Y axes, respectively. Control signals K_f^x, K_f^y can be formed so that vibration frequency along X and Y axes will be close to each other $\omega_1 \approx \omega_2 \approx \omega_r$ and $\Delta\omega \approx 0$. This is usually implemented by means of quadrature signal Q nulling using known procedure represented in [17]

$$Q = \pi(x\dot{y} - \dot{x}y) \to \text{null}. \quad (4)$$

Implementation of the procedure (4), for example, by means of proportional and integral (PI) controller leads to vibration of two channels X and Y at the same frequency ω_r. From the mathematical point of view it means that the following relationships are true

$$(k_{xx} - K_f^x D_x G_x)x + k_{xy}y \approx \omega_r^2 x,$$

$$(k_{yy} - K_f^y D_y G_y)y + k_{xy}x \approx \omega_r^2 y. \quad (5)$$

Substitution of the relationships (5) into the equation (3) allows obtaining of such expressions

$$\ddot{x} + d_{xx}\dot{x} + \omega_r^2 x = (2k\Omega - d_{xy})\dot{y} + K_d^x G_x \dot{x},$$

$$\ddot{y} + d_{yy}\dot{y} + \omega_r^2 y = (-2k\Omega - d_{xy})\dot{x} + K_d^y G_y \dot{y}. \quad (6)$$

As can be seen from the equations (6) frequencies of resonator vibrations on axes X and Y are the same. It means that control forces equalize resonator rigidities by these axes and compensate cross-coupling rigidity, which is characterized by coefficient k_{xy}. Interdependency of the equations (6) is defined by Coriolis forces and cross-coupling damping characterized by coefficient d_{xy}, which it is impossible to differ from Coriolis force that is angle rate. This causes the basic error of the vibratory gyro.

Stationary solution of the equations (6) can be represented in the following form

$$x = r\cos 2\theta \sin(\omega_r t);\ y = r\sin 2\theta \sin(\omega_r t + \varphi), \quad (7)$$

where φ is constant difference of phases between signals of electrodes X and Y; r is amplitude of standing wave; θ is angle between drive electrode X and standing wave antinode axis.

After substitution of the solution (7) in the equation (6) and some transformations it is possible to obtain

$$[d_{xx}\cos 2\theta - (2k\Omega - d_{xy})\sin 2\theta\cos\varphi - K_d^x G_x \cos 2\theta]\cos\omega_r t = (2k\Omega - d_{xy})\sin 2\theta \sin\varphi \sin\omega_r t,$$

$$[d_{yy}\sin 2\theta\cos\varphi + (2k\Omega + d_{xy})\cos 2\theta - K_d^y G_y \sin 2\theta\cos\varphi]\cos\omega_r t = (d_{yy}\sin 2\theta\sin\varphi - K_d^y G_y \sin 2\theta\sin\varphi)\sin\omega_r t. \quad (8)$$

As can be seen from the equations (8) the X and Y sense signals are amplitude modulated ones, where carrier is resonant frequency ω_r of the resonator and angle rate Ω together with measurement errors are modulating signals. Left and right sides of the equations (8) can be equal to each other at any instant of time if and only if amplitudes of the corresponding sine and cosine functions are equal to zero. Therefore, after transformation mechanical signals (displacements x and y) into electrical ones using transformation coefficients D_x and D_y of X and Y sense electrodes, respectively, four equations can be obtained after demodulation using two reference signals $\sin\omega_r t$ and $\cos\omega_r t$

$$-(2k\Omega - d_{xy})D_y \sin 2\theta\cos\varphi + D_x d_{xx}\cos 2\theta - K_d^x D_x G_x \cos 2\theta = 0,$$

$$(2k\Omega - d_{xy})D_y \sin 2\theta\sin\varphi = 0,$$

$$(2k\Omega + d_{xy})D_x \cos 2\theta + D_y d_{yy}\sin 2\theta\cos\varphi - K_d^y D_y G_y \sin 2\theta\cos\varphi = 0,$$

$$D_y d_{yy}\sin 2\theta\sin\varphi - K_d^y D_y G_y \sin 2\theta\sin\varphi = 0. \quad (9)$$

From the equations (9) it follows that when phase difference is equal to zero $\varphi=0$, only the first and third equations of the set (9) remain nonzero. In opposite case ($\varphi=\pi/2$) the stable standing wave can not be sustained.

Let us rewrite the first and third equations of the set (9) putting $\varphi=0$, as measurement equations

$$-2k\Omega D_y \sin 2\theta + D_x d_{xx}\cos 2\theta + d_{xy}D_y \sin 2\theta = z_x,$$

$$2k\Omega D_x \cos 2\theta + D_y d_{yy}\sin 2\theta + d_{xy}D_x \cos 2\theta = z_y. \quad (10)$$

where z_x and z_y are the X and Y sense axes measurement signals obtained after demodulation by the reference signal $\cos\omega_r t$.

From the equations (10) it follows that differential gyro gives us information about angle rate $-\Omega$ and Ω from X and Y sense electrodes, respectively. Coefficient of proportionality between angle rate and output signal is usually called the gyro scale factor. Differential gyro is characterized by two such coefficients by channels X and Y with appropriate notations SF_x and SF_y. Output signal components, which do not depend on the angle rate, are usually called the gyro zero bias. Differential gyro has also two biases by the X and Y channels with appropriate notations B_x, B_y. So, for introduced scale factors and biases it is possible to write the following expressions

$$SF_x = 2kD_y \sin 2\theta;\ B_x = D_x d_{xx}\cos 2\theta + d_{xy}D_y \sin 2\theta,$$

$$SF_y = 2kD_x \cos 2\theta;\ B_y = D_y d_{yy}\sin 2\theta + d_{xy}D_x \cos 2\theta. \quad (11)$$

It should be noted that zero biases and scale factors for both measuring channels are periodically changed in accordance with change of standing wave angle θ. Dependences of zero biases and scale factors on angle θ for both channels X and Y are represented in [12]. Thus equations for determination of angle θ_0, for which zero biases by channels X and Y will be equal, become

$$D_x d_{xx}\cos 2\theta_0 + d_{xy}D_y \sin 2\theta_0 = D_y d_{yy}\sin 2\theta_0 + d_{xy}D_x \cos 2\theta_0. \quad (12)$$

Solution of the equation (12) for θ_0 yields

$$\theta_0 = \frac{1}{2}\operatorname{atan}\frac{D_x}{D_y}\frac{d_{xx} - d_{xy}}{d_{yy} - d_{xy}}. \quad (13)$$

When the standing wave angle is θ_0, the difference of the two channel measurements $z_y - z_x$ cancels bias and increases angle rate signal. In this case, zero bias measurements can be obtained. For the most sensors $D_x \approx D_y$, $d_{xx} \approx d_{yy}$ and $d_{xy} << d_{xx}$, so $\theta_0 \approx \pi/8 = 22.5^o$.

When the standing wave angle is θ_0, the difference of the two channel measurements, $z_y - z_x$, cancels bias and increases angle rate signal. In this case, zero bias measurements can be obtained. For most sensors $D_x \approx D_y$, $d_{xx} \approx d_{yy}$, and $d_{xx} << d_{xy}$, so $\theta_0 \approx \pi/8 = 22.5^o$.

There is also standing wave angle θ^* that equalizes X and Y channel scale factors. This angle can be determined in the following way

$$2kD_y \sin 2\theta^* = 2kD_x \cos 2\theta^*,$$

$$\theta^* = \frac{1}{2}\text{a}\tan\frac{D_x}{D_y} = \frac{1}{2}\text{a}\tan\left(\frac{SF_y^\theta}{SF_x^\theta}\tan 2\theta\right), \quad (14)$$

where SF_x^θ, SF_y^θ are X and Y channel scale factors at arbitrary standing wave angle θ.

It should be noted that the angle θ^* is close to $\pi/8$. It is convenient in practice to perform the following actions:

– to set the initial value of the standing wave angle $\pi/8$;

– to determine SF_x and SF_y by using standard calibration procedure;

– to calculate θ^* using the expression (14);

– to form a control command for standing wave reorientation to the proper angular position θ^*.

When the standing wave angle is θ^*, the difference, $z_y - z_x$, and sum, $z_y + z_x$, of two X and Y channel measurement signals will be defined by the expressions

$$SF_d\Omega + (d_{yy} - d_{xx})\frac{D_xD_y}{\sqrt{D_x^2 + D_y^2}} = z_y - z_x,$$

$$\frac{D_xD_y}{\sqrt{D_x^2 + D_y^2}}(d_{yy} + d_{xx}) + \frac{D_y(D_x + D_y)}{\sqrt{D_x^2 + D_y^2}}d_{xy} = z_y + z_x,$$

$$SF_d = 4k\frac{D_xD_y}{\sqrt{D_x^2 + D_y^2}}. \quad (15)$$

The difference of both channels measurement does not contain damping cross-coupling d_{xy}, and the sum of the two channels does not contain angle rate and can be used for on-line estimation of bias parameters and differential CVG scale factor SF_d when k is known. It should be noted that scale factor SF_d does not depend on resonant frequency and vibration amplitude in contrast to CVG operating in conventional mode [16]. CVG output signals measurement results are presented in Fig. 4.

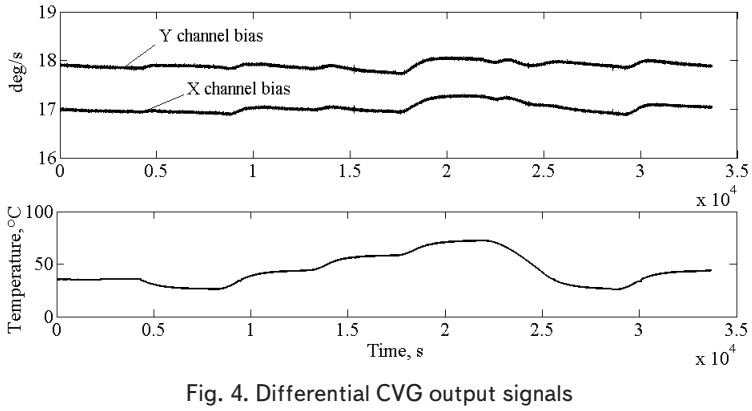

Fig. 4. Differential CVG output signals

The first two sub-graphs of Fig. 4 show high enough biases determined by d_{xx} and d_{yy} (see B_x and B_y in the expression (11)) from the point of view of equivalent angle rate. The third sub-graph shows close to zero bias of differential channel, because $(d_{yy} - d_{xx})/2 = -h\cos 2(\theta^* - \theta_\tau)$, and h is close to zero. The fourth sub-graph represents $z_y + z_x$ as a combination of differential CVG bias parameters in accordance with the expression (15). It is mainly determined by the large enough term $(d_{yy} + d_{xx})/2 = 2/\tau$.

4. 2. Inter-channel correlation matrix determination

In order to realize four signal processing techniques two types of measurements were made by the differential CVG prototype. The first type of measurements was made in static gyro position. X and Y channel biases raw measurement data in the temperature range (+26...+72) °C are shown in Fig. 5. Root mean square (RMS) value of noise deviation at temperature 72 °C for X channel signal is 0.019 deg/s, for Y channel signal it is 0.023 deg/s, and for differential channel it is 0.009 deg/s, respectively. X and Y channels raw data correlation matrix is

$$\text{corrcoef}(X,Y) = \begin{bmatrix} 1 & 0{,}769747 \\ 0{,}769747 & 1 \end{bmatrix}. \quad (16)$$

As can be seen from the expression (16) correlation coefficient $\rho = 0.769747$ is positive and far from optimal ρ_{opt} for n=2 ($\rho_{opt} = -1$). These measurement data are used to find temperature correction polynomial coefficients which then will be used to correct biases in the second type measurements at gyro rotation.

Fig. 6 shows raw dynamic (second type data) measurements at gyro rotation with angle rate ±50 deg/s. These measurements are an alternative to static, as shown in Fig. 5 temperature profile.

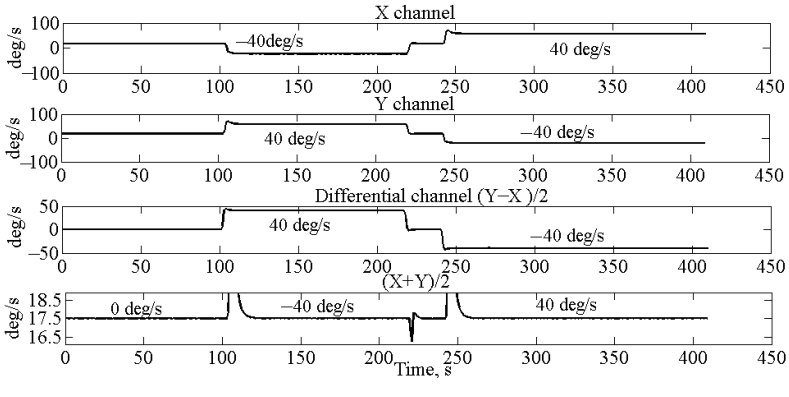

Fig. 5. Bias measurement in X and Y channels

It should be noted the fact that after correction of X and Y channel biases in the first type measurements, which results are shown in Fig. 7, the correlation matrix becomes equal to

$$\text{corrcoef}(X,Y) = \begin{bmatrix} 1 & -0{,}999546 \\ 0{,}999546 & 1 \end{bmatrix}. \quad (17)$$

As can be seen from the expression (17), after biases correction correlation coefficient $\rho = -0.999546$ is very close to $\rho_{opt} = -1$ for n=2. The fact that after biases correction correlation coefficient ρ becomes very close to ρ_{opt} has been verified and confirmed for another three prototypes of differential CVGs.

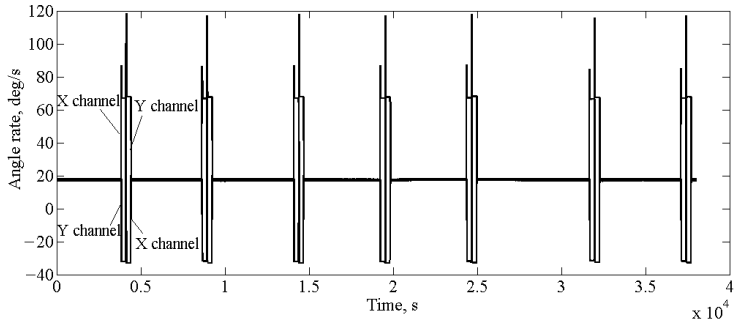

Fig. 6. X and Y channels angle rate measurement results

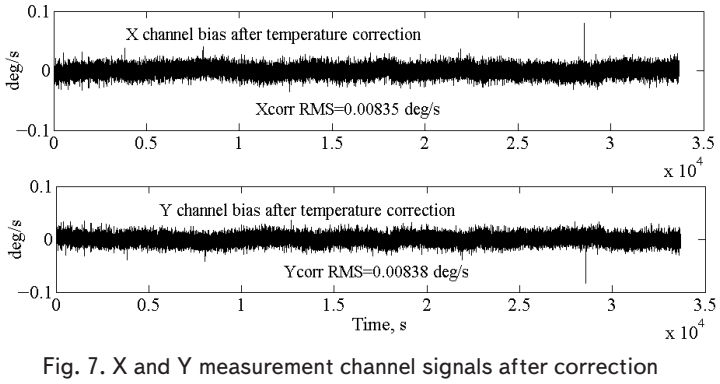

Fig. 7. X and Y measurement channel signals after correction

About 2 times reduction of RMS values of bias noise for X and Y channels (Fig. 7), as against data represented in Fig. 5, are due to that for bias correction both temperature sensor signal and internal control signals have been used. It should be noted that RMS value of bias noise for $z_y - z_x$ signal is almost the same with the value of 0.0093 deg/s.

5. CVG redundant information processing techniques research results

Differential CVG signals processing technique 1 is that bias polynomial model correction coefficients, obtained during preliminary testing are applied to each of X and Y measurement channels separately during rate measurements and then half difference of measurement results is taken.

Technique 2 is the same as technique 1, but correction is applied to the difference, $z_y - z_x$ of X and Y channel signals, i.e. the difference is firstly taken and then correction is applied to the difference signal that reduces computing load.

Technique 3 is that after X and Y signals correction (as it is made in technique 1) Kalman filter "virtual" gyro fusion algorithm is applied using 1st order Markov process as an angle rate model, realized in [3], with covariance matrix which normalized version is presented by the matrix (17). As a result the following system and measurement equations for "virtual" gyro are obtained

$$\Omega_{i+1} = -\Omega_i/\tau_\Omega + w_i; \quad \sigma_w^2 = 10; \ \tau_\Omega = 10^5; \Omega_0 = 0,$$

$$\vec{z}_{i+1} = H\Omega_{i+1} + \vec{v}_{i+1}; \ \vec{v}_i = \begin{pmatrix} v_i^1 & v_i^2 \end{pmatrix}^T; \ H = \begin{pmatrix} 1 & -1 \end{pmatrix}^T, \qquad (18)$$

where

$$R = E\left[\vec{v} \quad \vec{v}^T\right] = 10^{-4}\begin{bmatrix} 0{,}697613 & -0{,}699464 \\ -0{,}699464 & 0{,}701958 \end{bmatrix},$$

here $\vec{z}_{i+1} = (z_{i+1}^1 z_{i+1}^2)^T$ are X and Y channel measurement signals after biases correction; τ_Ω is a Markov process of the first order correlation time; $\vec{v}_i$ is X and Y channels white noise measurement vector; H is a measurement matrix; R is X and Y channels covariance matrix; Ω_0 is an initial value of angle rate.

Technique 4 of differential CVG signals processing is the same as technique 3, augmented by calculation of correlation matrix R in on-line manner after subtraction of estimated at previous sample time angle rate. As a result the following "virtual" gyro fusion algorithm is obtained:

$$R_{i+1} = (1-\alpha)R_i + \alpha(\vec{z}_{i+1} - H\hat{\Omega}_i - \vec{\mu}_i),$$

$$R_0 = \begin{pmatrix} 100 & 0 \\ 0 & 100 \end{pmatrix},$$

$$\vec{\mu}_{i+1} = (1-\alpha)\vec{\mu}_i + \alpha(\vec{z}_{i+1} - H\hat{\Omega}_i),$$

$$\vec{\mu}_0 = \begin{pmatrix} 0 & 0 \end{pmatrix}^T; \ \alpha = 10^{-4},$$

$$D_{i+1} = H^T R_{i+1}^{-1} H,$$

$$K = D_{i+1}^{-1}\left(-1/\tau_\Omega + \sqrt{\left(1/\tau_\Omega\right)^2 + D\sigma_w^2}\right)H^T R_{i+1}^{-1},$$

$$A = \exp\left(-1/\tau_\Omega - KHT\right),$$

$$\hat{\Omega}_{i+1} = A\hat{\Omega}_i + \left((A-1)/A\right)K\vec{z}_{i+1}, \qquad (19)$$

here $\vec{\mu}_i$ is X and Y channel signals mean value's vector; $\vec{\mu}_0$ is an initial value of μ variable; K is a Kalman filter gain coefficient; $\hat{\Omega}_i$ is angle rate estimate at *i*th time moment; T is a sample time.

Table 2 and Fig. 8 show constant 50 deg/s angle rate estimates obtained in the temperature range (+26...+72) °C for all four above mentioned processing techniques. Table 2 presents angle rate estimates after subtraction vertical component of the Earth angle rate, which is equal to 3.22×10^{-3} deg/s. Almost the same results are obtained for measurement of negative angle rate, –50 deg/s.

Table 2

Measurement results comparison based on four information processing techniques

Temperature, °C	Angle rate, deg/s			
	Technique 1	Technique 2	Technique 3	Technique 4
26.3	50.0821	50.1175	50.0819	50.0813
35.2	50.1334	50.1262	50.1332	50.1325
43.6	50.0818	50.0548	50.0817	50.0812
58.1	49.9761	49.9615	49.9759	49.9756
72.3	49.9889	50.0393	49.9887	49.9884
26.3	49.7441	49.7792	49.7439	49.7437
43.6	49.9404	49.9138	49.9403	49.9401
Mean	49.9924	49.9989	49.9922	49.9918
Std.	0.13	0.12	0.13	0.13
Random error	0.26 %	0.24 %	0.26 %	0.26 %
Systematic error	0.015 %	0.002 %	0.016 %	0.016 %

One can see from Table 2 that random errors for all compared techniques are close to each other. The systematic er-

ror of technique 2 is much lower than that of techniques 1, 3, and 4. Systematic and random errors of techniques 1, 3 and 4 are very close to each other when measuring angle rate in the temperature range.

Within the framework of the research it is convenient to compare bias noise during and between angle rate measurements, when there is a temperature ramp and, also, transient during angle rate change. Table 3 presents RMS value of noise when angle rate is present and absent at 72 °C stable temperature.

Data of Table 3 show that technique 4 has RMS noise almost 2 times less than that of other techniques. It should be noted that using Table 3 data one can calculate angle rate short term fluctuation s_W as follows

$$\sigma_\Omega = \sqrt{(0{,}00817)^2 - (0{,}00805)^2} = \\ = 0{,}0014 \text{ deg} / \text{s}. \qquad (20)$$

Fig. 9 shows overshoot processes when changing angle rate abruptly from 0 to 50 deg/s. Overshoot for technique 1 is 4 %, for 2 is 2.9 %, for 3 is 2.5 % and for 4 is 1.3 %. Thus, technique 4 has almost 2 times lower overshoot, than the best of three others.

Table 3

RMS values of noise at stable temperature 72 °C

Experiment conditions	RMS value, deg/s			
	Technique 1	Technique 2	Technique 3	Technique 4
Angle rate is present	0.00817	0.00818	0.00769	0.00460
Angle rate is absent	0.00805	0.00806	0.00756	0.00435

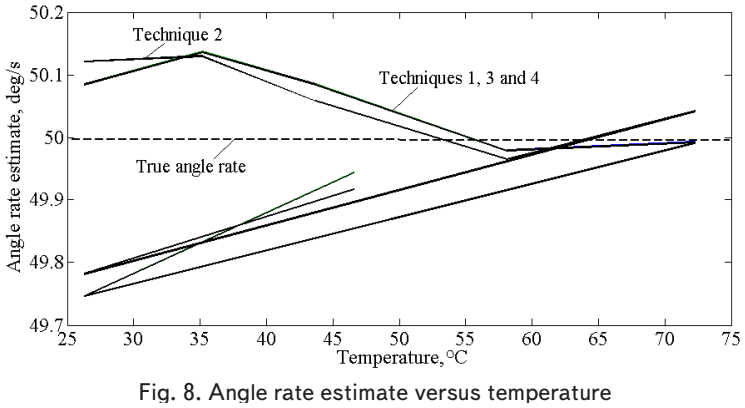

Fig. 8. Angle rate estimate versus temperature

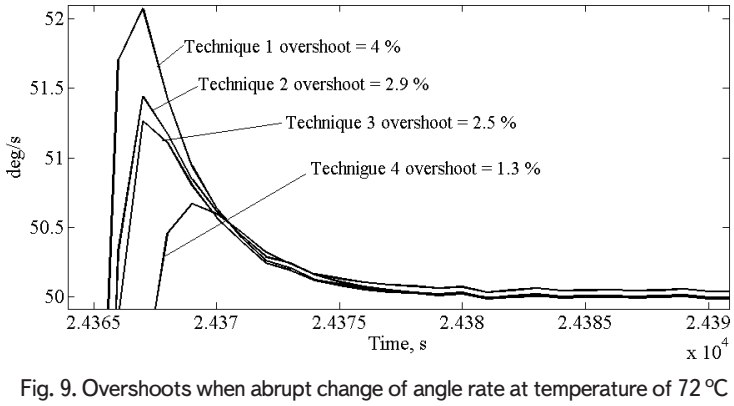

Fig. 9. Overshoots when abrupt change of angle rate at temperature of 72 °C

Fig. 10 shows the root of Allan variances of X and Y biases between angle rate measurements when temperature changes from 72 °C to 26 °C at ramp −0.6 °C/min.

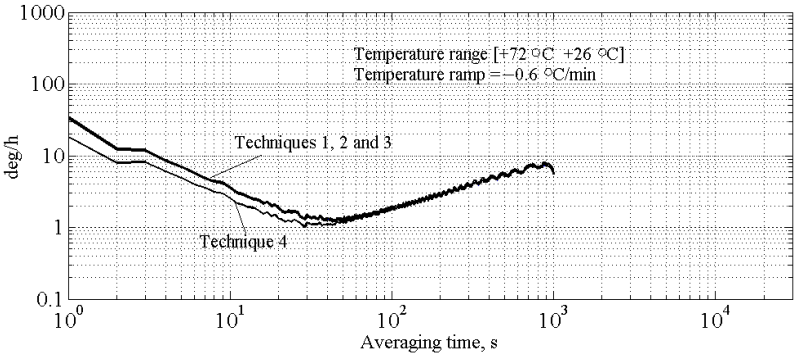

Fig. 10. Root of Allan variances for all four techniques

Noise parameters for all four techniques during temperature ramp do not significantly differ. Allan curves of the first three techniques have no visible difference. Technique 4 has 20–30 % less quantum noise, random walk and bias instability than others.

6. Discussion of redundant information processing techniques results

Differential CVG was created by Ukrainian specialists that have been carried out experimental researches [10] and have been shown the possibility to realize CVG with three modes of operation [12] along with rate and rate-integrating ones. Advantages and disadvantages of the differential mode are now carried out. The goal of these works is to define conditions of switching to this operating mode to provide maximum working and operating characteristics of triple-mode CVG in comparison with two other modes.

Based on carried out researches, the possibility to use the known algorithm of "virtual" gyro in differential CVG was revealed. This algorithm was grounded in [9] and applied to an array of four one-axis unidirectional gyros created on the basis of MEMS gyro [7]. This algorithm is designed for redundant information processing. It is shown, that using the modified algorithm of "virtual" gyro in differential CVG, it is possible to provide correlation coefficient close to optimal value. This leads to sufficient measurement noise decrease and also to improvement of overshoot when abrupt change of angle rate, that it is important for CVG applications in high dynamics vehicles. Nevertheless the systematic component of angle rate is not improved. Furthermore, measurement noise is decreased due to significantly greater quantity of computing operations resulting in computational burden increase. Thus, it is convenient to use the considered algorithm in differential CVG information processing in systems for stabilization of lines-of-sight of devices operated on ground vehicles. As a rule, such systems are sensitive to noise influence but do not require accurate determination of angle rate in contrast to the navigation systems.

7. Conclusions

1. The modified algorithm of "virtual" gyro is proposed. In contrast to [3, 8] this algorithm calculates inter-channel correlation matrix in on-line manner. This decreases measurement errors due to taking in account changes of inter-channel correlation coefficient versus time.

2. The comparative analysis of the developed modified algorithm of measuring information processing (technique 4) with other known techniques (1, 2 and 3) is carried out. This analysis has been shown that the algorithm of technique 4 has approximately twice lesser RMS random error both during angle rate measurement and without it (bias measurement).

3. Conditions, for which differential CVG inter-channel coefficient is close to the optimal value $\rho_{opt}=-1$ when the number of redundant channels is equal to 2, are determined. These conditions are implementation of scale factor and bias temperature correction in differential CVG.

4. It is defined that the systematic error of angle rate measurement by means of technique 2 is almost one order of magnitude lower in comparison with systematic errors of other techniques. Also it is shown by means of quantitative estimation that technique 4 during abrupt change of angle rate provides almost 2 times lower overshoot in comparison with three others.

References

1. Chikovani, V. V. Trends of Ukrainian All Digital Coriolis Vibratory Gyroscopes Development [Text]: conference / V. V. Chikovani // Institute of Electrical & Electronics Engineers (IEEE). – Kiev, 2014. – P. 25–28. doi: 10.1109/msnmc.2014.6979720
2. Wang, W. Design of a novel MEMS gyroscope array [Text] / W. Wang, X. Lv, F. Sun // Sensors. – 2013. – Vol. 13, Issue 2. – P. 1651–1663. doi: 10.3390/s130201651
3. Xue, L. Analysis of Dynamic Performance of a Kalman Filter for Combining Multiple MEMS Gyroscopes [Text] / L. Xue, L. Wang, T. Xiong, C. Jiang, W. Yuan // Micromachines. – 2014. – Vol. 5, Issue 4. – P. 1034–1050. doi: 10.3390/mi5041034
4. Ting, T. O. State-of-Charge for Battery Management System via Kalman Filter [Text] / T. O. Ting, K. L. Man, C.-U. Lei, C. Lu // Engineering Letters. – 2014. – Vol. 22, Issue 2. – P. 75–82.
5. Chaudhuri, S. S. Vision Based Target-Tracking Realized with Mobile Robots using Extended Kalman Filter [Text] / S. S. Chaudhuri, A. Konar // Engineering Letters. – 2007. – Vol. 14, Issue 1. – P. 176–184.
6. Jiang, C. Signal Processing of MEMS Gyroscope Arrays to Improve Accuracy Using a 1st Order Markov for Rate Signal Modeling [Text] / C. Jiang, L. Xue, H. Chang, G. Yuan, W. Yuan // Sensors. – 2012. – Vol. 12, Issue 12. – P. 1720–1737. doi: 10.3390/s120201720
7. Liu, J. Signal Processing Technique for Combining Numerous MEMS Gyroscopes Based on Dynamic Conditional Correlation [Text] / J. Liu, Q. Shen, W. Qin // Micromachines. – 2015. – Vol. 6, Issue 6. – P. 684–689. doi: 10.3390/mi6060684
8. Ji, X. Research on Signal Processing of MEMS Gyro Array [Text] / X. Ji // Mathematical Problems in Engineering. – 2015. – Vol. 2015. – P. 1–6. doi: 10.1155/2015/120954
9. Patent No. US 10/383,475. High Accuracy Inertial Sensors from Inexpensive Components [Text] / Bayard D. S., Ploen S. R. – No. 6882964 B2, declared: 06.03.2003; published: 19.04.2015.
10. Chikovani, V. V. The Compensated Differential CVG [Text] / V. V. Chikovani, T. O. Umakhanov, P. I. Marusyk // In Proceedings of Symposium Gyro Technology. – University of Karlsruhe, Germany, 2008. – P. 3.1–3.8.
11. Patent No. 95709. MPK. G01C 19/02. Metod vimiryuvannya kutovoi shvidkosti Koriolosovim vibratsiynim giroskopom [Text] / Chikovani V. V. – No. a201001344, declared: 25.08.2011; published: 26.06.2013, Buyl. № 16.
12. Chikovani, V. V. Differential Mode of Operation For Multimode Vibratory Gyroscope [Text]: conference / V. V. Chikovani, H. V. Tsiruk // Institute of Electrical & Electronics Engineers (IEEE). – Kiev, 2015. – P. 87–90. doi: 10.1109/apuavd.2015.7346568
13. Trusov, A. A. Non-Axisymmetric Coriolis Vibratory Gyroscope With Whole Angle, Force Rebalance, and Self-Calibration [Text] / A. A. Trusov, D. M. Rozelle, G. Atikyan, S. A. Zotov, B. R. Simon, A. M. Shkel, A. D. Meyer // Solid-State Sensors, Actuators and Microsystems. – Workshop Hilton Head Island, South Carolina, 2014. – P. 419–422.
14. Gregory, J. Characterization and Control of a High-Q MEMS Inertial Sensor Using Low-Cost Hardware [Text]: conference / J. Gregory, J. Cho, K. Najafi // Institute of Electrical & Electronics Engineers (IEEE). – Myrtle Beach, S.C., 2012. – P. 239–247. doi: 10.1109/plans.2012.6236886
15. Chikovani, V. V. Differential mode of operation for ring-like resonator CVG [Text]: conference / V. V. Chikovani, O. A. Suschenko // Institute of Electrical & Electronics Engineers (IEEE). – Kiev, 2014. – P. 451–455. doi: 10.1109/elnano.2014.6873426
16. Lynch, D. D. Coriolis Vibratory Gyros [Text] / D. D. Lynch // In Proceedings of Simposium Gyro Technology. – University of Karlsruhe, Germany, 1998. – P. 1.1–1.14.
17. Lynch, D. D. Vibratory gyro analysis by the method of averaging [Text]: conference / D. D. Lynch // Gyroscopic Technology and Navigation. Scientific Council of the Russian Academy of Sciences on the Traffic Control and Navigation Problems. – Sankt-Peterburg, 1995. – P. 26–34.